# Distinct functions for ERK1 and ERK2 in cell migration processes during zebrafish gastrulation

Krens, S.F.G.; He, S.; Lamers, G.E.M.; Meijer, A.H.; Bakkers, J.; Schmidt, T.; ... ; Snaar-Jagalska, B.E.
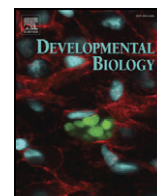
# Distinct functions for ERK1 and ERK2 in cell migration processes during zebrafish gastrulation

S.F. Gabby Krens [a,*], Shuning He [a], Gerda E.M. Lamers [a], Annemarie H. Meijer [a], Jeroen Bakkers [c,d], Thomas Schmidt [b], Herman P. Spaink [a], B. Ewa Snaar-Jagalska [a,*]

[a] Institute of Biology, Leiden University, Wassenaarseweg 64, 2333 AL Leiden, The Netherlands
[b] Physics of Life Processes, Leiden Institute of Physics, Leiden, Niels Bohrweg 2, 2333 CA, Leiden University, The Netherlands
[c] Hubrecht Laboratory, Uppsalalaan 8, 3584 CT Utrecht, The Netherlands
[d] Interuniversity Cardiology Institute for the Netherlands, Catharijnesingel 52, 3501 DG Utrecht, The Netherlands

## ARTICLE INFO

## ABSTRACT

The MAPKs are key regulatory signaling molecules in many cellular processes. Here we define differential functions for ERK1 and ERK2 MAPKs in zebrafish embryogenesis. Morpholino knockdown of ERK1 and ERK2 resulted in cell migration defects during gastrulation, which could be rescued by co-injection of the corresponding mRNA. Strikingly, *Erk2* mRNA cross-rescued ERK1 knockdown, but *erk1* mRNA was unable to compensate for ERK2 knockdown. Cell-tracing experiments revealed a convergence defect for ERK1 morphants without a severe posterior-extension defect, whereas ERK2 morphants showed a more severe reduction in anterior–posterior extension. These defects were primary changes in gastrulation cell movements and not caused by altered cell fate specification. Saturating knockdown conditions showed that the absence of FGF-mediated dual-phosphorylated ERK2 from the blastula margin blocked initiation of epiboly, actin and tubulin cytoskeleton reorganization processes and further arrested embryogenesis, whereas ERK1 knockdown had only a mild effect on epiboly progression. Together, our data define distinct roles for ERK1 and ERK2 in developmental cell migration processes during zebrafish embryogenesis.

© 2008 Elsevier Inc. All rights reserved.

## Introduction

The mitogen-activated protein kinase (MAPK) cascade governs key signaling pathways that control cell proliferation, differentiation and survival responses in all eukaryotes. Altered MAPK signaling is associated with developmental defects and various pathologies, including cancer. The MAPK cascade involves sequential activation of a serine/threonine kinase (MAPKKK), followed by a dual-specific MAPK kinase (MAPKK) and a dual-phosphorylated MAPK target. The vertebrate family of MAPKs consists of three major subfamilies: ERK, JNK and p38 (Johnson and Lapadat, 2002). An important challenge is to understand the complexity of the different MAPK cascades. Although specificity of these cascades has been reported (Kolch, 2005), it is clear that crosstalk occurs and strong indications for redundancies exist (Johnson et al., 2005). Distinct cellular functions in cancer formation have recently been shown for ERK1 and ERK2, which are the most intensively studied MAPKs of the ERK subfamily (Lloyd, 2006). For example, tumorigenicity of transplanted NIH 3T3 cells stably expressing an oncogenic form of Ras in nude mice was largely inhibited by co-transfection of ERK1, but not by ERK2 or p38 (Vantaggiato et al., 2006).

The canonical pathways of ERK1/2 activation are well studied in vitro and different animal models have been used to address ERK1 and ERK2 functions in development. However, due to their crucial roles in early embryogenesis, the differential functions of ERK1 and ERK2 are not yet clearly defined. FGF and MEK signaling are necessary for the formation of notochord and mesenchyme cells during ascidian embryogenesis (Kim and Nishida, 2001). In *Drosophila*, FGF-dependent ERK activation was shown to be required for proper mesoderm dispersal (Gabay et al., 1997; Gryzik and Muller, 2004; Stathopoulos et al., 2004; Wilson et al., 2005). In chick, functions of activated ERK1/2 in axon growth were suggested (Kato et al., 2005). In *Xenopus*, ERK2 was shown to be required for mesoderm differentiation (Gotoh et al., 1995) and neural specification (Umbhauer et al., 1995; LaBonne et al., 1995; Uzgare et al., 1998). Studies using knockout mice clearly indicated that ERK1 and ERK2 have distinct functions. Gene disruption of *erk2* is lethal during early development, showing that ERK1 is not redundant to ERK2 (Yao et al., 2003). In contrast, *Erk1*−/− mice are viable, fertile and of normal size. However, the proliferation and maturation of the thymocytes is affected, despite expression of ERK2 (Pagès et al., 1999). Elevated ERK2 activation was observed in primary neurons isolated from *erk1* knockout mice, whereas no higher ERK2 levels were detected in the brain. Mouse embryos lacking exon 2 of the *erk2* gene die *in utero* before embryonic day (E) 8.5 due to a defect in trophoblast development. *Erk2*-deficient mice fail to form the

* Corresponding authors. Fax: +31 71 5274999.
E-mail addresses: S.F.G.Krens@biology.leidenuniv.nl (S.F.G. Krens),
B.E.Snaar-Jagalska@biology.leidenuniv.nl (B.E. Snaar-Jagalska).

ectoplacental cone and the extra-embryonic ectoderm (Saba-El-Leil et al., 2003), and also fail to form mesoderm, based on histological criteria at E6.5 and E7.5 (Yao et al., 2003). Finally, ERK2 is critical for proliferation of the trophoblast stem-cell population, which is essential for placenta formation (Ornitz and Itoh, 2001).

In this study we aimed to increase the understanding of the differential roles of ERK1 and ERK2 in early vertebrate embryogenesis and cell migration processes, using the zebrafish model. Because of its *ex utero* development the zebrafish model is optimally suitable to study the link between the cellular and developmental functions of ERK1 and ERK2. Previously, immuno-histochemical analysis of the spatio-temporal patterns of ERK1/2 phosphorylation showed that, like in mouse (Corson et al., 2003) and chick (Delfini et al., 2005), zebrafish ERK1/2 is activated locally during segmentation stages (Shinya et al., 2001; Sawada et al., 2001). Furthermore, it was shown that insulin-like growth factors (IGFs) stimulated zebrafish cell proliferation by activating ERK-MAPK and PI3-kinase signaling pathways (Pozios et al., 2001). Subsequently, research on the ERK-MAPK pathway in zebrafish development has mostly concentrated on the functions of the FGF/MAPK pathway, which also contains the inhibitors Sef (Furthauer et al., 2002; Tsang et al., 2002), Sprouty2/4 and the MAPK phosphatases MKP1 and MKP3 (Tsang et al., 2004). Over-activation of the FGF/ERK-pathway led to dorsalized embryos by inhibiting expression of *bmp* genes (Furthauer et al., 2004). In contrast, over-expression of ERK-MAPK phosphatase MKP3 or injection of a high dose of mRNA of the inhibitor Sef resulted in an opposite ventralization (Furthauer et al., 2002; Tsang et al., 2004).

Recently, we identified the zebrafish orthologs of the MAPK gene family and determined their specific spatial and temporal expression patterns during zebrafish embryogenesis (Krens et al., 2006). We showed that the zebrafish genome encodes all members of MAPK-subfamily, ERK, JNK and p38, and that *erk1* and *erk2* are differentially expressed compared to each other and to the other members of the zebrafish *mapk* gene family.

Here, we report on knockdown studies of ERK1 versus ERK2 and present evidence for their differential effects on convergence extension (CE) cell movements. Cell-tracing experiments showed that ERK1 morphants displayed reduced convergence cell movements, whereas ERK2 morphants showed a more severe reduction in anterior–posterior extension of the dorsal body axis, without significantly altering the early cell fate specification. Stringent knockdown conditions for ERK2 arrested embryogenesis at the onset of epiboly, thereby preventing the blastula to gastrula transition. Taken together, our data imply distinct functions for ERK1 and ERK2 MAPKs in gastrulation cell migration during zebrafish embryogenesis. We also examined the function of FGF signaling at the onset of epiboly by the use of several inhibitors of the FGF/Ras/MAPK signaling cascade, such as the chemical FGF receptor inhibitor SU5402, dominant negative forms of the FGFR1 and 4 and dominant negative hRas (RasN17). In SU5402-treated embryos, the induction of epiboly was affected in the same way as in ERK2 morphants and led to the depletion of active ERK2 signal from the margin. This indicates that FGF-mediated ERK2 activation in the margin plays a key-role in epiboly progression.

## Materials and methods

### Cloning

Total RNA was isolated from adult Tuebingen zebrafish, using TRIZOL® Reagent protocol (Invitrogen). cDNA for zebrafish ERK1 and ERK2 genes was cloned into pCR®4Blunt-TOPO® (Invitrogen) using primers flanking the coding region, based on EST AB030902 and AB030903, and subcloned in the pCS2+ vector using the EcoR1-site. Constructs were checked by sequence analysis.

### Micro-injection of morpholinos and mRNAs

One-cell stage embryos were injected with 1 nl of the solubilized compounds in 1× Danieau's buffer [58 mM NaCl, 0.7 mM KCl, 0.4 mM MgSO₄, 0.6 mM Ca(NO₃)₂, 5.0 mM HEPES; pH 7.6] containing 1% phenol red solution (Sigma). At the 1K-stage (3 hpf), embryos with phenol red in the animal pole were selected as positive-injected embryos. Definition of stages was according to Kimmel et al. To block translation of the ERK1 or ERK2 mRNA morpholinos were targeted against the 5′-UTR of the respective mRNAs (GeneTools Philomath, OR, USA): ERK1MO, 5′-TCTGTCCGCAAATCGTCGCCTTCGC; ERK2MO, 5′-CACCCAAAAGCACCAGGAAAAGCTC (0.2 mM or 0.4 mM).

Synthetic mRNA encoding zebrafish *erk1* and *erk2* genes, human *RasN17* (Deng and Karin, 1994), *Xenopus* XFD (Shinya et al., 2001) or *Xenopus* bΔFR4 (Hongo et al., 1999) was transcribed with SP6 RNA polymerase using the mMessage mMachine Kit (Ambion), using linearized pCS2+ constructs.

### Pharmacological inhibition of FGF signaling

To inhibit FGFR activity, embryos were treated with SU5402, (Mohammadi et al., 1997) (Calbiochem) at 40 μM in defined E2 embryos medium at 28.5 °C in the dark (Furthauer et al., 2004).

### Cell tracing

Embryos were (co-)injected at the one-cell stage with 0.3% 4,5-dimethoxy-2-nitrobynzyl (DMND)-caged fluorescein dextran (molecular mass 10,000; Molecular probes, gift from Hammerschmidt lab). Uncaging was performed as previously described (Bakkers et al., 2004) with UV light at shield stage (6 hpf) using a Zeiss axioplan microscope, with 40× objective and adjustable pinhole. Embryos were imaged at 6, 8 and 10.5 hpf. The dorsal convergence and anterior extension angles were measured using Image J (NIH imaging software).

### Whole-mount immuno-staining

Embryos were fixed overnight in 4% paraformaldehyde at 4 °C. Embryos were washed and incubated for 2 h in blocking buffer (PBS, 0.1% BSAc, 1% Triton X100). After overnight incubation at 4 °C with 1:100 dilution of primary antibody (Polyclonal phospho-p44/42 MAPK antibody from Cell Signaling; total ERK antibody K-23, Santa Cruz Biotechnology) in blocking buffer, embryos were washed with blocking buffer, and incubation for 1 h in 1:100 diluted secondary antibody (Goat anti-rabbit Alexa 488 conjugated). Embryos were washed in blocking buffer and three washes in PBS containing 1% Triton X-100.

### Whole-mount in situ hybridization

Embryos were fixed overnight in 4% paraformaldehyde in PBS at 4 °C and in situ hybridization was performed as described previously (Thisse et al., 1993) using the described probes.

### Protein isolation and western blot analysis

Embryos were dechorionated and de-yolked in Ca/Mg free solution. Cells were pelleted and washed with PBS followed by a passive lysis in buffer (0.125% NP40, 25 mM Tris–HCl, 2 mM EDTA, 1 mM Na3VO4, 25 mM NaF and 1 complete mini EDTA-free protease inhibitor cocktail tablet (Roche) per 10 ml lysis-buffer). Protein extract was analyzed by western blotting, using phosphor-specific and total ERK antibody (Snaar-Jagalska et al., 2003).

## Results

Immuno-histochemical analysis of the localization of active/phosphorylated ERK1 and ERK2 MAPK showed elevated levels of ERK phosphorylation in the cleavage furrows at the 16 cell stage, in the margin during epiboly and gastrulation, and at locations of neural differentiation (anterior neural boundary and mid-hindbrain boundary, Fig. S1) and segmentation (Pozios et al., 2001; Shinya et al., 2001; Sawada et al., 2001). Immuno-histochemistry cannot distinguish between ERK1 and ERK2. However, we recently showed that *erk1* and *erk2* display differential spatio-temporal expression patterns during zebrafish development (Krens et al., 2006), suggesting distinct functions for ERK1 and ERK2 during zebrafish development.

### Morpholino knockdown of ERK1 and ERK2 results in specific phenotypes

To elucidate the functions of ERK1 and ERK2 in zebrafish development, gene-specific morpholinos (MO) directed to the 5′ untranslated sequences, were used to block the translation of *erk1* or *erk2* mRNAs. Injection of 0.2 mM ERK1MO or ERK2MO induced severe developmental defects (Fig. 1), while treatment with the same concentration of the standard control MO had no effect (data not shown).

At 24 hpf approximately 10% of ERK1MO injected embryos were dead, and 85% ($n$=130) displayed phenotypes characterized by a shorter body axis and somites without the distinct v-shape (Fig. 1A). In contrast, ERK2MO injected embryos ($n$=75) showed approximately 70% lethality at 24 hpf and 85% at 48 hpf (Fig. 1E) and the surviving ERK2MO morphants showed more severe phenotypes than the ERK1 morphants. At 24 hpf, the head was still distinguishable and the dev-

elopment of tail structures was severely defected (Fig. 1B), resulting in shortened phenotypes at 48 hpf (Fig. 1G) and somites structures to be barely recognizable. Approximately 50% of ERK1MO-injected and 15% ERK2MO-injected embryos survived up to 48 hpf (Fig. 1E). The surviving morphants were shortened at 24 and 48 hpf and had enlarged heart-cavities (Figs. 1F, G). Protein analysis of the surviving embryos by western blot using a general ERK antibody showed that
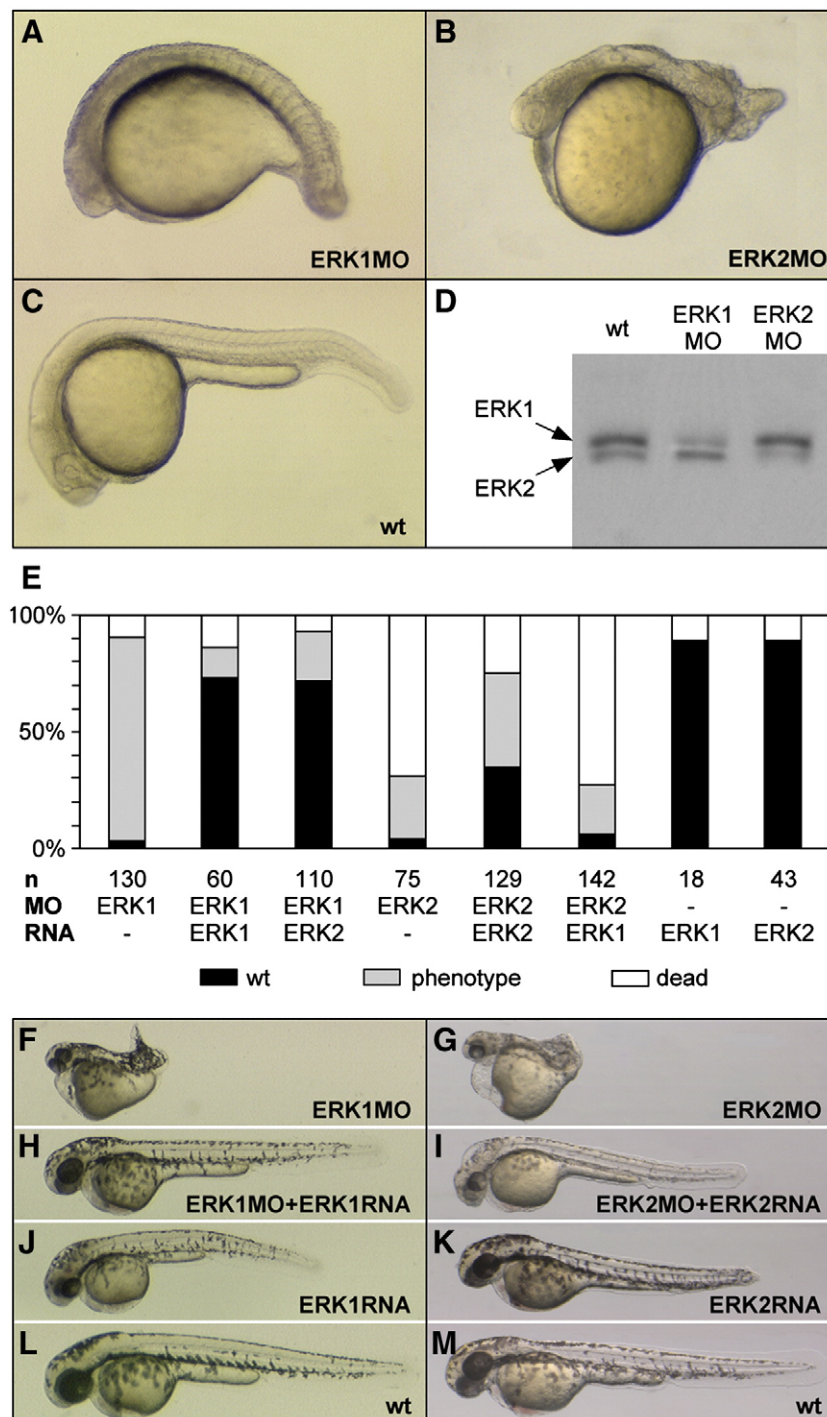


**Fig. 1.** Specific ERK1 and ERK2 knockdown by morpholino injection. (A–C) Images show representative examples of the ERK1 (A) or ERK2 (B) knockdown phenotypes at 24 hpf, compared to wild type (wt) embryos (C). (D) Specific knockdown was confirmed by Western blot analysis optimized to discriminate between the sizes of ERK1 (p44MAPK) and ERK2 (p42MAPK) protein and detected with global ERK antibody (D). Protein samples were isolated from 20 hpf embryos, injected with 0.2 mM ERK1MO or ERK1MO. (E) Statistics of ERK knockdown and (cross-) rescue experiments determined by co-injection of ERK1 or ERK2 morpholino with synthetic *erk1* or *erk2* mRNA at 24 hpf. Black = wild type; gray = phenotype; white = dead. (F–M) Images show phenotypes of surviving knockdown embryos at 48 hpf (F, G), embryos rescued by co-injection of corresponding mRNA (8pg *erk1* RNA, 1.5pg *erk2* RNA) (H, I), embryos injected with mRNA only (J, K) and wild type embryos at 48 hpf (L, M).

ERK1 and ERK2 protein levels were specifically and significantly reduced by the respective ERK1 and ERK2 morpholinos (Fig. 1D).

To test the specificity of the obtained knockdown phenotypes, rescue experiments were performed using synthetic *erk1* and *erk2* mRNAs lacking the MO target site. Protein samples were made at the shield stage from embryos injected with 100 pg mRNA and western blot analyses showed that the synthetic mRNAs were correctly translated into proteins and were dual-phosphorylated/activated in the embryo (Fig. S2B). For rescue experiments mRNA concentrations were used below those that induced over-expression phenotypes (Fig. S2). Co-injection of synthetic *erk1* mRNA (8 pg/embryo) with 0.2 mM ERK1MO rescued 67% of embryos with the shorter body axis at 24 hpf and 50% at 48 hpf (Figs. 1E, H). Co-injection of *erk2* mRNA (1.5 pg/embryo) with 0.2 mM ERK2MO increased the percentage of survivors from ~20% to more than 70% at 24 hpf and rescued the body axis defect in ~35% of the embryos (Figs. 2E, I). The redundancy of the ERK1 and ERK2 was determined in cross-rescue experiments using the same mRNA concentrations as described above (Fig. 2E and data not shown). ERK1 knockdowns were rescued by co-injection of *erk2* mRNA with similar efficiency as by *erk1* mRNA. Co-injection of ERK2MO with *erk1* mRNA did not increase the number of surviving embryos nor rescued the body axis defects, indicating that the amount of *erk1* mRNA that rescued ERK1 knockdown cannot cross-rescue the ERK2 knockdown phenotype.

*Distinct functions for ERK1 and ERK2 in gastrulation cell movements*

The low surviving rates and the severe phenotypes of ERK1 and ERK2 morphants at 24 hpf indicate possible roles for these kinases in earlier developmental processes. To address this, ERK1MO and ERK2MO injected embryos were closely monitored at yolk plug closure (YPC) to tailbud stages (Figs. 2A–F). ERK1MO-injected embryos showed rather normal extension (distance between arrowheads) compared to control embryos (Figs. 2A, B), but showed a widening of the notochord (Figs. 2D, E). Strikingly, ERK2MO-injected embryos showed a shortened anterior–posterior axis at the end of gastrulation (Fig. 2C), but a far less severe effect on the widening of the notochord (Fig. 2F), than ERK1MO-injected embryos.
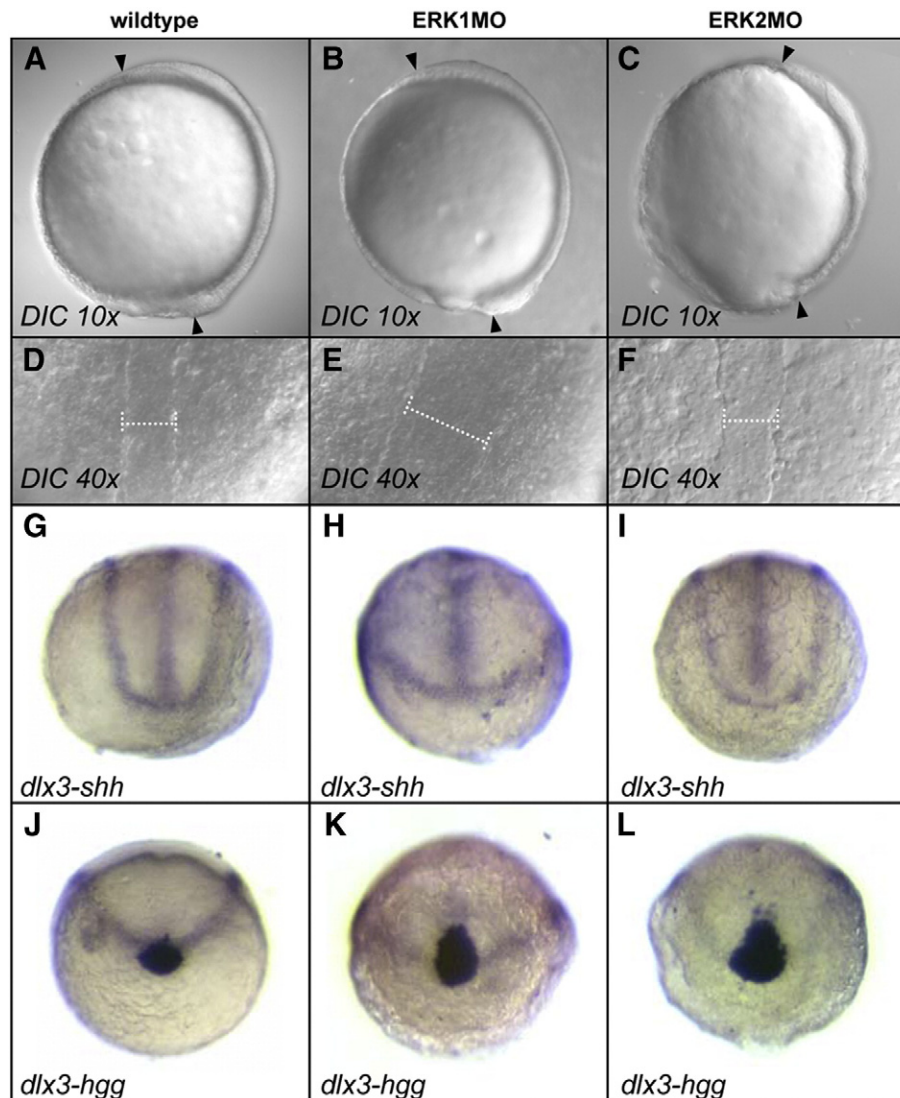


**Fig. 2.** Phenotypic characterization of ERK1 and ERK2 morphants in late-gastrulation and early segmentation indicates affected cell migration in CE movements. (A, D, G, J); wild type control embryos, (B, E, H, K); ERK1 knockdown embryos, injected with 0.2 mM ERK1MO, (C, F, I, L); ERK2 knockdown embryos, injected with 0.2 mM ERK2MO. (A–C); Live embryos at yolk plug closure (YPC) to tailbud (TB) stages, animal pole is up, dorsal to right in wild type, ERK1MO or ERK1MO injected embryos, The distance between the arrowheads resembles the length of the AP body axis (Zeiss EC Plan-Neofluar 10×/0.30 objective), or dorsal view (D–F), white spacer highlights the widening of the dorsal notochord (Zeiss Plan-Neofluar 40×/0.75 ∞/0.17 objective). (G–L); Combined in situ hybridization on 10-hpf old embryos with *dlx3* (edge neural plate) with *shh* (midline) or with *hgg1* (hatching gland) marker genes (anterior view, dorsal to top).

These results indicated possible effects of ERK1 and ERK2 knockdown on dorsal–ventral patterning or CE cell movements. We first addressed this question by in situ hybridization using the marker genes *dlx3*, expressed in the neural plate, *sonic hedgehog* (*shh*), expressed in the notochord, and *hgg1*, expressed in the developing hatching gland, in 10 hpf embryos (Figs. 2G–L) as previously described (Jopling and den Hertog, 2005). In ERK1 morphants, the *dlx3*-expression domain was much wider and the hatching gland was located more posterior (Figs. 2H, K). Strikingly, ERK2 morphants did not show this widening of the neural plate (*dlx3*), suggesting that this defect was ERK1MO specific. In ERK2 morphants (Figs. 2I, L), the *shh* expression domain in the midline was not fully extended in the anterior direction, resulting in a gap between the *dlx3* and *shh* expression

domains. In addition, the expression domain of *hgg1* was located even more posterior than in ERK1morphants, indicating affected extension cell movements in ERK2 morphants.

### Knockdown of ERK1 or ERK2 perturbs gastrulation cell movements differently

In order to directly study the specific effect of ERK1 and ERK2 knockdown on cell movements during gastrulation, we performed cell-tracing experiments using DMNB-caged fluorescent dextran (Kozlowski et al., 1997; Sepich et al., 2000). To follow convergence (dorsal) cell migration, lateral mesoderm cells located 90° from the dorsal shield, were labeled by uncaging the fluorophore with a local-
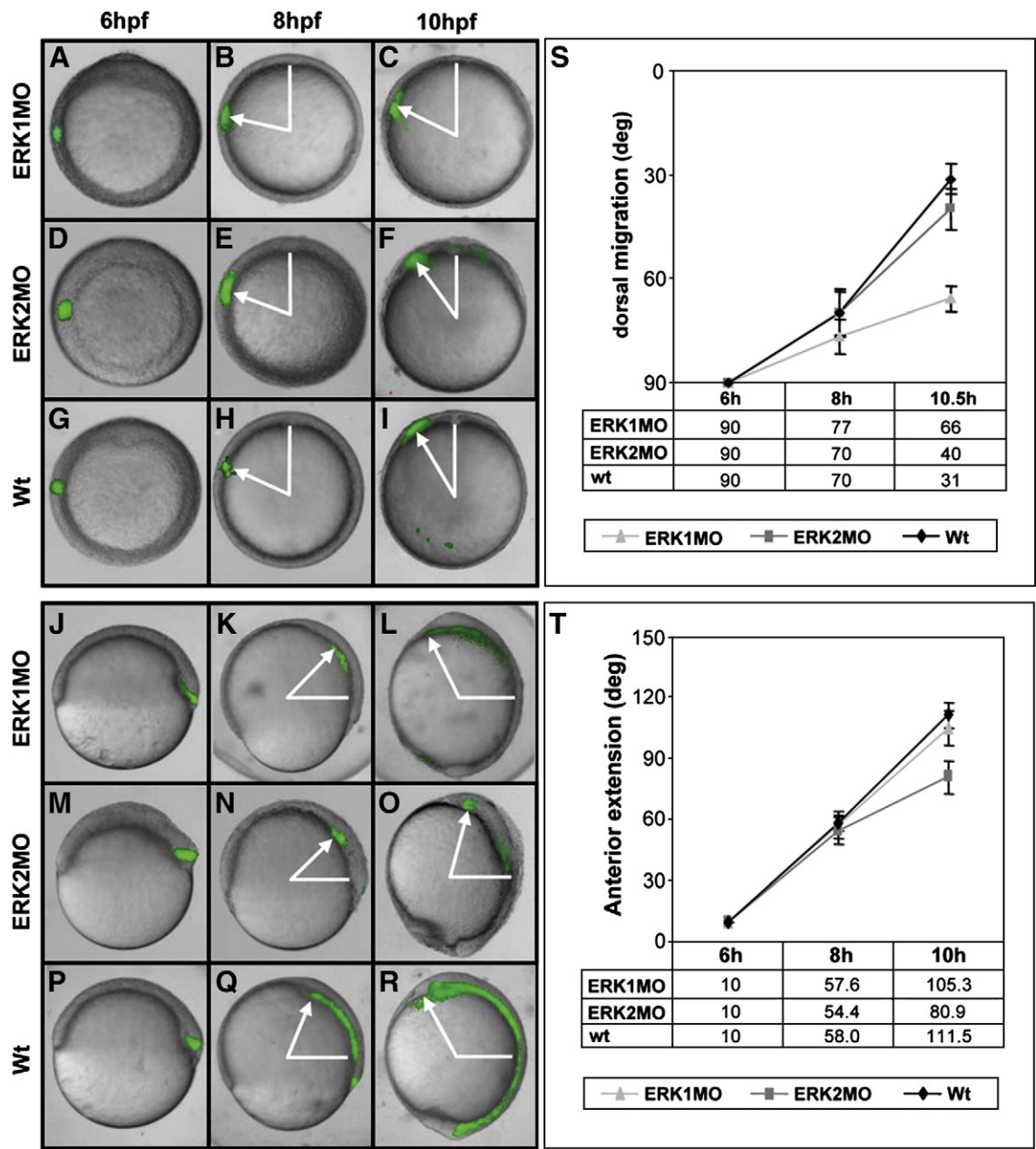


**Fig. 3.** ERK1 and ERK2 are differentially involved in CE cell movements. Embryos were injected with MO and caged fluorescein dextran, which was activated at shield stage (6 hpf) laterally to determine dorsal migration (A–I; animal pole view, dorsal to top) and dorsally to determine anterior extension (J–R; lateral view, dorsal to right). Images show uncaging cells directly after activation (A, D, G, J, M, P), at 8 hpf (B, E, H, K, N, Q) and at 10 hpf (C, F, I, L, O, R). Cell-tracing experiments were performed in ERK1MO injected (A–C, J–L), ERK2MO injected (D–F, M–O) and wild type embryos (G–I, P–R). (S) Quantification of dorsal migration (*n* = 10), measured as indicated with white arrows (A–I) as degrees from dorsal. (T) Quantification of anterior migration measured as indicated with white arrows (J–R) as degrees of anterior movement (*n* = 10). ERK1MO: gray triangle, ERK2MO: dark gray square, wild type: black diamond.

ized pulse of ultraviolet light at 6 hpf and followed in time (Figs. 3A–I, S). Extension cell migration processes were monitored by labeling cells in the dorsal shield (Figs. 3J–R, T).

The cell-tracing experiments showed that ERK1 morphants displayed a severely reduced movement of the labeled lateral cells towards the dorsal axis in time (Figs. 3A–C), while in ERK2 morphants only a slight reduction of dorsal migration was observed (Figs. 3D–F). In contrast, ERK2 morphants showed greatly reduced extension movements (Figs. 3M–O) compared to extension movements in wild type (Figs. 3P–R) and ERK1MO-injcted embryos (Figs. 3J–L). Quantification of 10 embryos indicated that the reduction of dorsal migration for ERK1 knockdown (Fig. 3S) and the reduced anterior extension migration for ERK2 knockdown (Fig. 3T), were significant, and confirms the previous suggestions based on the in situ results (Fig. 2). To address if the observed phenotypes in ERK1 and ERK2 knockdown embryos were primary cell movement defects or secondary effects due to a patterning alteration we performed in situ hybridization experiments with several different marker genes and observed no patterning defects (Fig. S3). Together, these results indicate differentially affected CE movements by ERK1 and ERK2 knockdown.

*ERK1 depletion mildly affects epiboly progression, whereas ERK2 depletion causes a developmental arrest at the onset of epiboly*

Taken into account that the knockdown of ERK1 and ERK2 was not completely saturated (Fig. 1D), we applied more stringent knockdown conditions by doubling the MO concentration and studied the effects on epiboly (Figs. 4 and S4). Embryos injected with 0.2 mM ERK1MO (Figs. S4A, B) did not show any obvious phenotype until 80% epiboly, while doubling the concentration to 0.4 mM slightly delayed epiboly compared to wild type embryos (Fig. S4G). Embryos injected with 0.2 mM ERK2MO were delayed to 65% epiboly at 8 hpf (Figs. 4 and S4C), when wild type embryos reached 80%. Knockdown of ERK2 by injection of 0.4 mM ERK2MO prevented epiboly in 38% (Fig. 4 — arrest category and Fig. S4D) of the injected embryos and inhibited epiboly progression and further entrance into gastrulation stages in 46% of the embryos (Fig. 4 severe). This effect was rescued by co-injection of 20 pg synthetic *erk2* mRNA (Fig. S4E), which resulted in 82% (49 from 60 embryos) of the co-injected embryos entering gastrulation. Injection of this amount of synthetic *erk2* mRNA did not induce any phenotype by itself, at this stage.

To further address the functional redundancy between ERK1 and ERK2, we knocked down both genes at the same time by co-injection of 0.2 mM ERK1MO and 0.2 mM ERK2MO. Double morphant embryos also showed defects in epiboly. However the penetrance of the epiboly phenotype was lower than for the single

0.4 mM ERK2 morphants (65%, $n = 132$ versus 82%, $n = 103$) and in situ hybridization with *ntl* revealed that double morphant embryos still formed some axial mesoderm (data not shown). Considering that analysis of double morphant embryos does not clarify distinct roles, but more the global functions of ERK1/2 signaling, we did not follow up on the double morphant analysis.

To analyze the active ERK signal at early epiboly, phospho-ERK immune-localization was analyzed by pixel-intensity and sectioning (Fig. 5), revealing that in addition to the strong phospho-ERK signal in the margin, active ERK is also present in the rest of the animal pole (gray-value plot in Fig. 5A). The strongest signal was detected at the putative dorsal side of the margin at this stage (Fig. 5B). Sectioning of embryos stained for active ERK1/2 at oblong, sphere, dome, 30%-, 40%- and 50% epiboly demonstrates phospho-ERK presence in the EVL from oblong–sphere stage onwards (Figs. 5C–H). Phospho-ERK was detected in deep cells in the margin from dome stage onwards (Figs. 5E–H, with magnification in E′ and H′).

Nomarski microscopy was performed to study the affected epiboly initiation at 4.5 hpf (Figs. 6A–F). The leading edge of the migrating cells in the margin and the EVL cells in wild type embryos (Figs. 6A, D) and ERK1MO embryos (Figs. 6B, E) showed a sharp front migrating over the yolk. Knockdown of ERK2 induced a discontinuity in the margin and delayed crowding of the yolk syncytial nuclei (YSN) in the external yolk syncytial layer (YSL), resulting into a broadened YSL (Figs. 6C, F).

We performed immuno-histochemistry against the dual-phosphorylated ERK1/2 at 4.5 hpf and 8 hpf (Figs. 6G–I,J–L). In the control embryos (Figs. 6G, J) and the ERK1MO injected embryos (Figs. 6H, K) phosphorylated ERK was still detected in the margin in both stages. However, ERK phosphorylation was completely abolished in ERK2MO injected embryos (Figs. 6I, L) at both stages, indicating that ERK2 is the active ERK MAPK in the margin during gastrulation cell movements and that ERK2 plays a key-role in epiboly progression.

As previously described in studies using *Xenopus* and mice, ERK2 is required for mesoderm differentiation (Gotoh et al., 1995; Yao et al., 2003). Therefore the expression of the mesoderm markers *ntl* (brachyury in *Xenopus*) and *tbx6* in both ERK1 and ERK2 morphants was tested (Figs. 6M–R). In ERK1 morphants we observed a slight reduction of *ntl* and *tbx6* expression in the margin, where *ntl* expression stayed strongly expressed at the putative dorsal side, and *tbx6* expression was diminished at this site (Figs. 6N, Q). In ERK2 morphant, *ntl* and *tbx6* expression was almost absent (Figs. 6O, R), showing impaired mesoderm differentiation (Yao et al., 2003).

Experimental evidence in *Fundulus* demonstrated that the YSL is still able to epibolize when the overlying blastoderm and EVL are
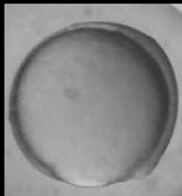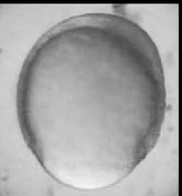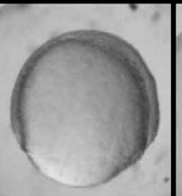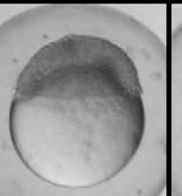


| | n | wt | light | mild | severe | arrested | dead |
|---|---|---|---|---|---|---|---|
| ERK2MO (0.2mM) | 95 | 0% | 20% | 55% | 15% | 3% | 7% |
| ERK2MO (0.4mM) | 96 | 0% | 0% | 13% | 46% | 38% | 4% |
| wt | 44 | 100% | 0% | 0% | 0% | 0% | 0% |

**Fig. 4.** Classification of phenotypes of embryos injected with 0.2 mM or 0.4 mM ERK2MO, compared to wild type embryos at 8–9 hpf. Classification into wild type, light, mild, severe and arrested phenotype categories is indicated by percentages.

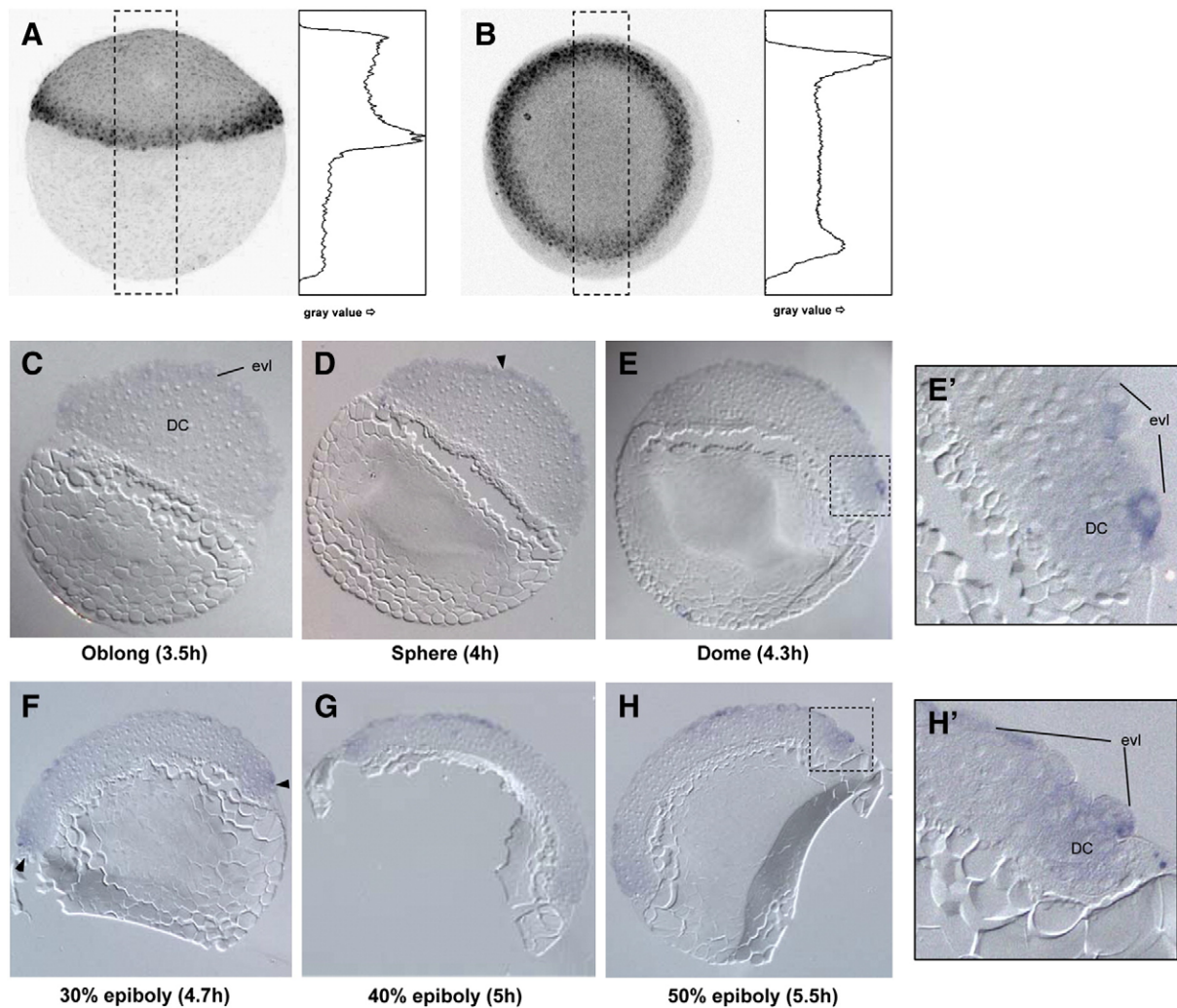**Fig. 5.** Active ERK is localized in the EVL prior epiboly and detected in EVL and marginal deep cells upon epiboly initiation. Embryos were fixed and subsequently stained for ERK activation by immuno-fluorescence at 30% epiboly (A, lateral view, dorsal to right and panel B, top view, dorsal to top) and quantified by pixel-intensity plots (gray-value in graphs). The phospho-ERK signal was weakly detected in the whole animal pole and stronger in the margin, with the strongest signal in the putative dorsal margin (B). Sectioning of embryos AP-stained for active ERK1/2 at epiboly initiation: oblong, sphere, dome, 30%-, 40%- and 50% epiboly (C–H respectively; lateral view of 8 μm section, images with Zeiss EC Plan-Neofluar 10×/0.30 objective, presumptive dorsal to right), revealed that phospho-ERK is present in the EVL from oblong–sphere stage onwards (C–H). Phospho-ERK was detected in deep cells in the margin from dome stage onwards (E–H, with magnification in panel E′ and H′). Arrowheads indicate initial detection of the signal (EVL in panel D, ventral and dorsal margin in panel F).

removed. This indicates that YSL epiboly can still occur in embryos lacking mesoderm (Betchaku and Trinkaus, 1978). The migration of the YSN to the vegetal pole is considered as a driving force through all stages of epiboly (Kane et al., 1996), next to radial intercalation (Myers et al., 2002; Montero and Heisenberg, 2004; Solnica-Krezel, 2006). At late blastula stages, the YSL forms a broad band and contains most of the YSN. At sphere/dome stage, the wide belt of external YSL narrows in the animal-vegetal direction and the YSN become increasingly crowded. When the blastoderm expands vegetally, reaching 30% epiboly, the YSN of the external YSL concentrate near the EVL at the margin (Solnica-Krezel and Driever, 1994). To follow migration of the YSN *in vivo*, 10 μM SYTOX-green nucleic acid stain was (co-)injected in wild type control embryos and morpholino-treated embryos (Figs. 7A–F). At 8 hpf, the YSN of control embryos were at 80% epiboly (Fig. 7D), whereas the YSN of ERK1 morphants were delayed at 50% epiboly (Fig. 7E). In ERK2 morphants the YSN were located at the top of the yolk at 8 hpf and did not show any migration towards the vegetal pole (Fig. 7F), leading to the conclusion that the depletion of activated ERK2 from the margin prevents YSL-migrating to the vegetal pole.

To initiate crowding of the YSN at sphere/dome stage, the microtubule network of the external YSL contracts and becomes denser at the margin (Solnica-Krezel and Driever, 1994). The

immuno-histochemistry of tubulin (Figs. 7G–L) revealed a narrow band of microtubules in the YSL in wild type embryos (Fig. 7G, enlarged in Fig. 7J) and ERK1MO injected embryos (Figs. 7H, K). In ERK2MO injected embryos (Figs. 7I, L) narrowing of the microtubules of the YSL did not occur, revealed by the broader YSL in the ERK2 depleted embryos.

The actin cytoskeleton within the YSL and EVL also fulfills an important role during epiboly as it has been shown that the disruption of the actin-based structures leads to the slowing or immediate arrest of epiboly (Cheng et al., 2004). In a study by Köppen et al., it was indicated that cell shape at the epithelial margin is of critical importance. The movement of the outer epithelium (EVL) over the yolk cell surface involves the contraction of the marginal cells. This process depends on the recruitment of actin and myosin2 within the yolk cytoplasm along the margin of the enveloping layer (Köppen et al., 2006).

To address whether the cell shape and the recruitment of actin to the blastula margin was affected, we stained the embryos with Alexa568-labeled phalloidin (Figs. 7M–R). Enriched phalloidin-staining was observed within the YSL along the EVL margin in wild type (Figs. 7M, P) and ERK1MO injected embryos (Figs. 7N, Q). In ERK2 morphants this enrichment was clearly weaker (Figs. 7O, R).
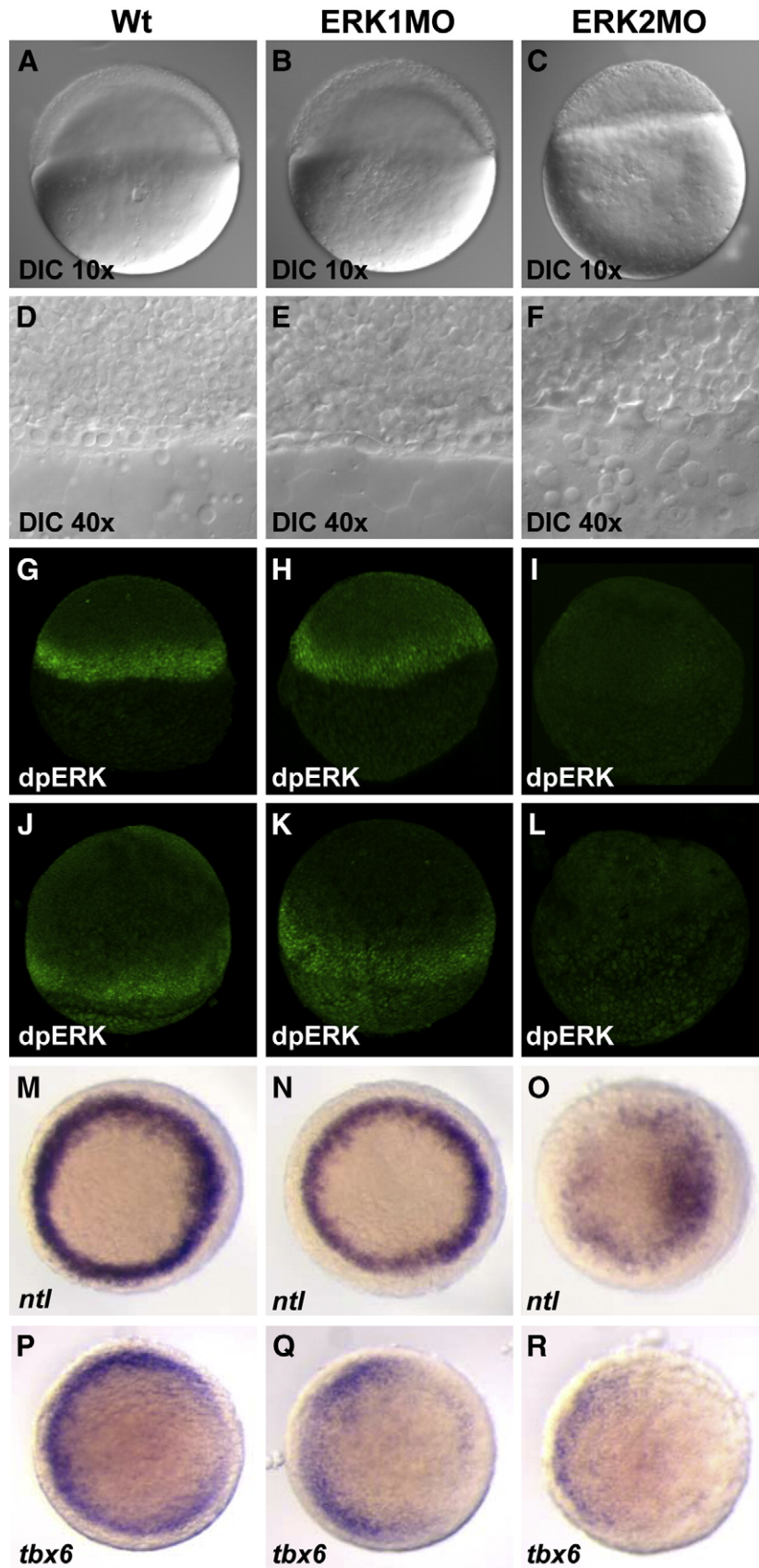
**Fig. 6.** Saturating knockdown of ERK2 prohibits epiboly initiation and revealed ERK2 to be the active MAPK in the margin. Embryos were injected with 0.4 mM ERK1MO (B, E, H, K, N, Q) or ERK2MO (C, F, I, L, O, R) and compared to wild type embryos (A, D, G, J, M, P). Nomarski/differential interference contrast (DIC) microscopy using a Zeiss EC Plan-Neofluar 10×/0.30 objective (A, B, C) and a Zeiss Plan-Neofluar 40×/0.75 ∞/0.17 (D, E, F) was used to monitor the margin at the onset of gastrulation (4.5 hpf). Localization of dpERK was detected by immuno-localization in wild type, ERK1MO and ERK2MO injected embryos at 4.5 hpf (G–I) and 8 hpf (J–L) by phospho-specific ERK antibody. Images in panels G–L were taken by confocal laser scanning microscopy. Mesoderm formation was followed using in situ hybridization markers *ntl* (M–O) and *tbx6* (P–R), top view, presumptive dorsal side right.
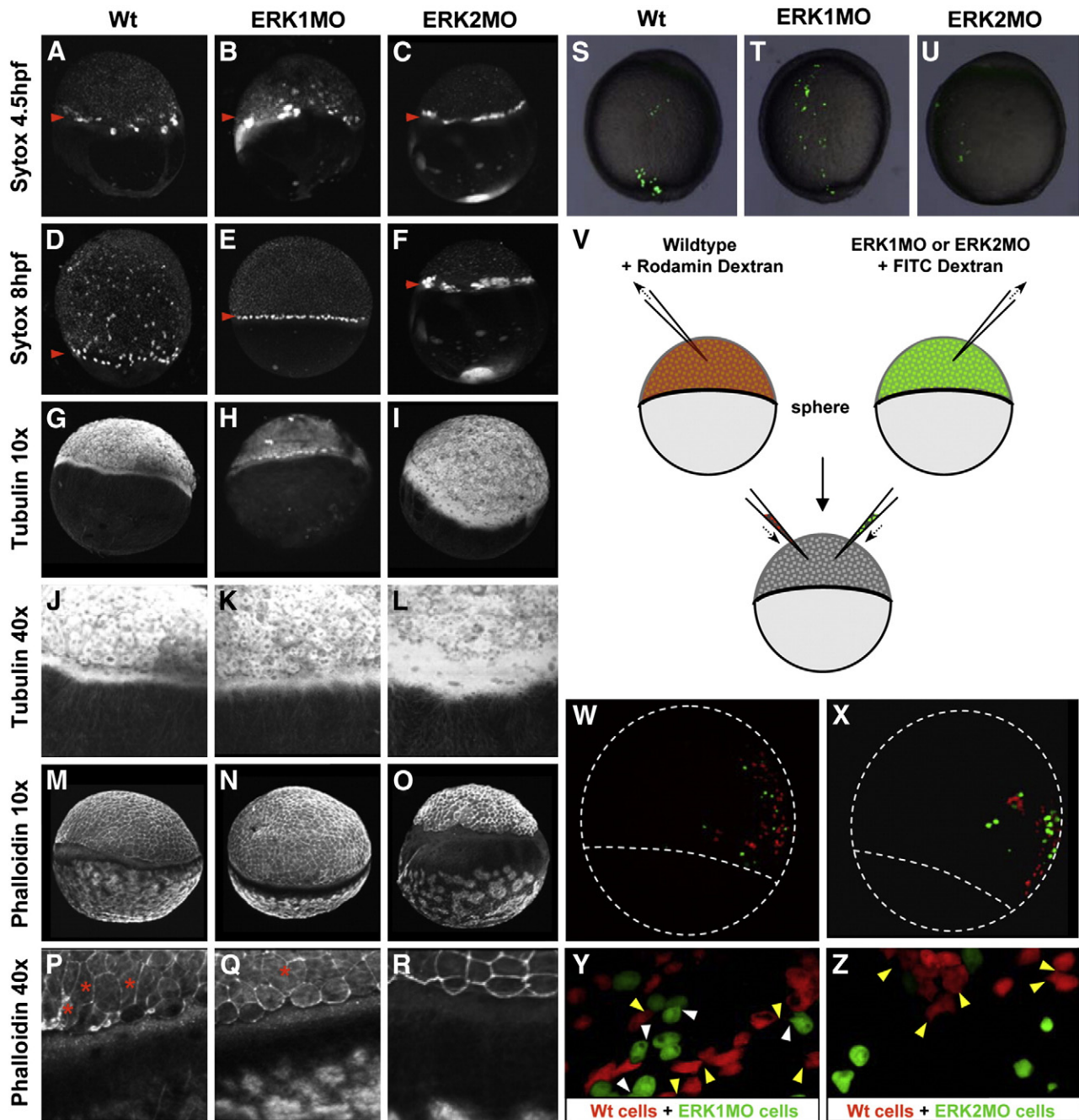
**Fig. 7.** Depletion of active ERK2 affects migration of the YSL, cytoskeleton reorganization and cell shape. (A–F) YSL-migration was followed *in vivo* by co-injection of 10 mM sytox green at 4.5 hpf (A–C) and 8 hpf (D–F). The animal-to-vegetal migration of the YSN within the YSL is indicated with a red arrowhead. The YSL of ERK2 morphants does not migrate to the vegetal pole in time (C, F) as in wild type embryos (A, D) or ERK1 morphants (B, E; slightly delayed). (G–L) Tubulin cytoskeleton was analyzed by antibody staining (G–I, Zeiss EC Plan-Neofluar 10×/0.30 objective; J–L, Zeiss Plan-Neofluar 40×/0.75 ∞/0.17). Tubulin structures nicely condensate at the vegetal base of the YSL in wild type embryos (G, J) and ERK1 morphants (H, K), but this is perturbed in ERK2 morphants (I, L). (M–R) Actin cytoskeleton was analyzed by Phalloidin staining (M–O, 10× objective; P–R, 40× objective). Local actin recruitment in the YSL is observed in both wild type (M,P) and ERK1 morphants (N, Q), but not in ERK2 morphants (O, R). The red asterisks indicate stretched cells, only observed in wild type and ERK1 morphants. (S, T, U); lateral view, dorsal to right. FITC dextran-labeled wild type, ERK1MO or ERK2MO is transplanted into wild type hosts and grown to complete epiboly. (V); Schematic representation of a double transplantation experiment. Wild type embryos are injected with Rhodamin dextran, morphant embryos are co-injected with FITC dextran. Embryos are grown till sphere stage and cells from both donor embryos are transplanted into the anima pole of a wildtype acceptor embryo and let to develop. (W, X) Overlay of images taken by confocal laser scanning microscopy of co-transplanted wild type (red) and ERK1 or ERK2 morphant cells (green) into wild type hosts at approximately 7 hpf, with enlargements in (S, T). Yellow arrowheads indicate filopodia formation by wild type cells; white arrowheads indicate filopodia formation by morphant cells (only in panel S). Dotted lines in panels W and X indicate epiboly progression and the outline of the embryo.

The cell shape of wild type cells showed protrusive activity and stretched cells were observed in both wild type and ERK1 morphants (to a lesser extend), but not in ERK2 morphants (Figs. 7P–R, red asterisks).

To test if the epiboly defect could be due to arrested development rather than to specific defects in morphogenesis, we performed transplantation experiments (Figs. 7S–Z). FITC-labeled morphant cells transplanted to a wild type host were still able to undergo epiboly, but at tail bud stage ERK2 morphant cells were found not to have migrated as far to the vegetal pole when compared to ERK1 morphant or wild type transplanted cells (Figs. 7S–U).

Double cell transplantations were performed to determine their relative positioning and if affected cell shapes as observed in
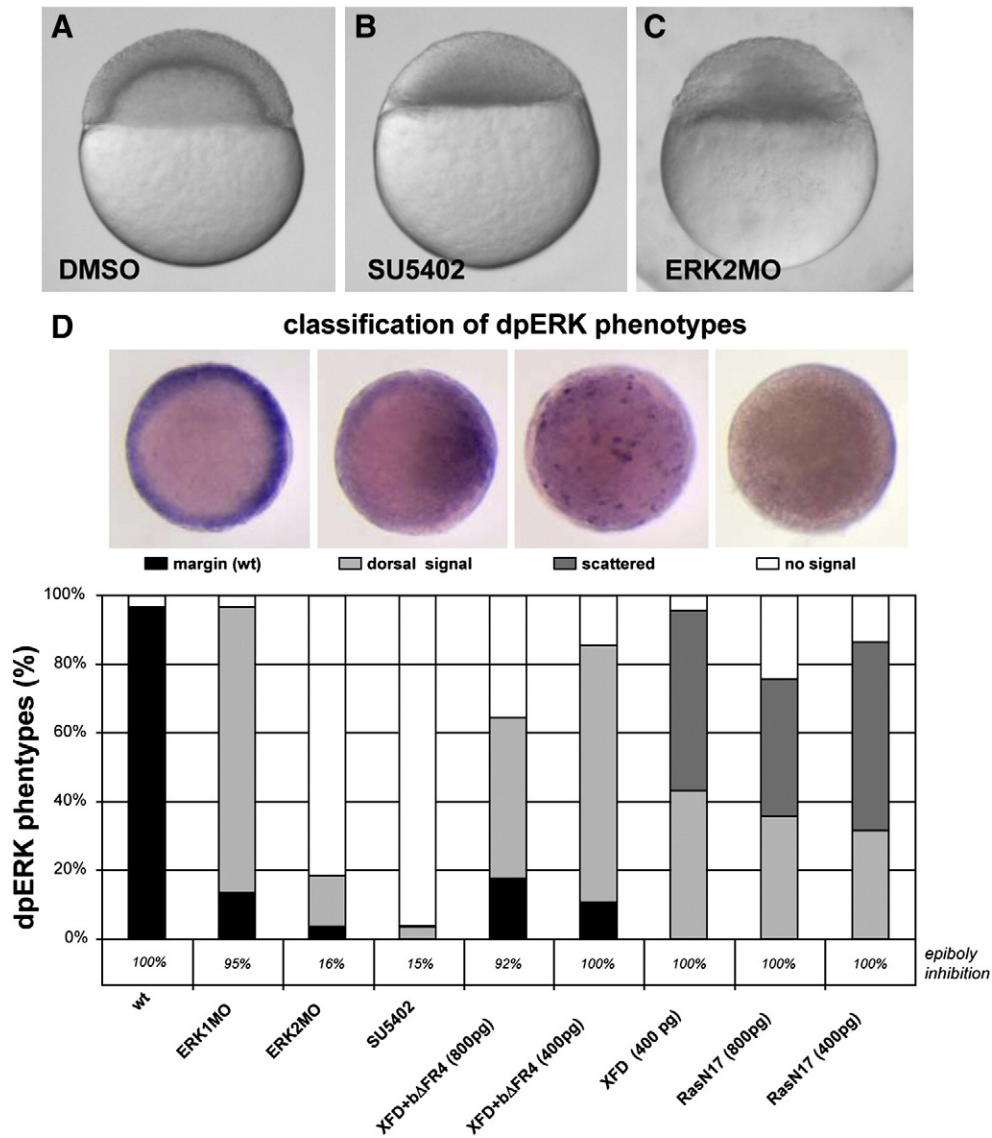
**Fig. 8.** Chemical inhibition of FGF signaling phenocopies ERK2MO affects and prevents epiboly initiation. Representative embryos treated with DMSO (A), SU5402 (B) or injected with ERK2MO (C). Both SU5402 (40 μM) treated and ERK2 depleted embryos do not initiate epiboly, whereas (co-)injections of synthetic mRNA encoding XFD and bΔFR4 (800 or 400 pg total, ratio 1:1), XFD only (400 pg) or Ras N17 (800 or 400 pg) did not affect epiboly initiation significantly (D; percentages indicated below the graph). (D) Injected or SU5402 treated embryos were analyzed for active ERK signaling (dpERK) after the mentioned treatment, at 4 hpf. The observed dpERK phenotypes were imaged from the top and classified in 4 groups; staining in the margin like in wild type conditions (wt; black), depletion of dpERK from the margin, but still present at the putative dorsal side (dorsal signal; light gray), no signal in the margin, but scattered pattern of cells expressing dpERK (scattered; dark gray) and no signal detected (white). The different phenotypes were scored per treatment and the percentages were plotted in a graph (D).

Figs. 7P, Q, R were cell autonomous. FITC-labeled cells from ERK1 or ERK2 morphant were co-transplanted with rhodamin-labeled wild type cells into a wild type host at sphere stage (Fig. 7V) and imaged at 8 hpf (Figs. 7W, X). These studies confirmed that ERK2 morphant cells were less efficient in epiboly compared to wildtype and ERK1 morphant cells migration (Figs. 7W, X). The transplanted wild type cells showed clear stretching and the formation of filopodia. These features were reduced in ERK1 morphant cells (green cells in S) and completely absent in ERK2 morphant cells (green cells in T), indicating that this effect was cell autonomous. Together, these data suggest that ERK morphant cells are affected in their migration properties, but not completely impaired. The observed ERK2 phenotype probably caused by combined cell migration and cytoskeleton reorganization defects.

To exclude a proliferation defect due to the depletion of functional ERK1 or ERK2 protein, phosphorylated histone H3 was used as a proliferation marker (Fig. S5). The presence of phospho-histone H3 was assayed in wild type and morphants at 30% (Figs. S5A–C) and 80%

(Figs. S5D–F) epiboly and embryos were counterstained with phalloidin to outline the embryos. Phosphorylated histone H3 was detected in all embryos tested and indicates that proliferation was still present in ERK1 (Figs. S5B, E) and ERK2 (Figs. S5C, F) morphants at both time points. We also performed in situ cell-death staining by TUNEL (Figs. S5G–K) to determine if apoptosis was induced by either the knockdown of ERK1 or ERK2. In the ERK2MO arrested embryos some positively stained cells were found at 8 hpf, however the apoptosis-related nuclear fragmentation was not observed (data not shown). Knockdown of ERK1, like in the wild type embryos, did not show any apoptosis at this stage.

*Chemical inhibition of FGF signaling phenocopies the ERK2MO phenotype and prevents epiboly initiation*

To address the possible involvement of FGF signaling as one of the predominant activators of ERKs during development, we performed
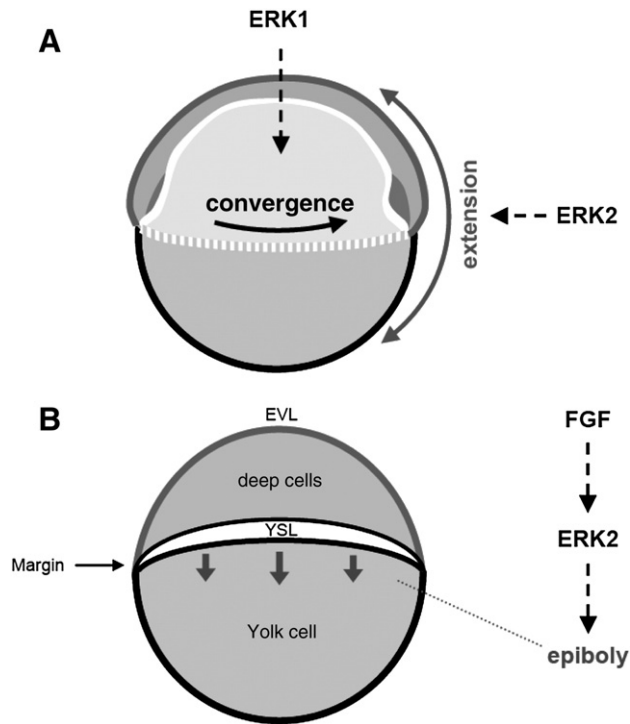
**A**

ERK1

convergence

extension

ERK2

**B**

EVL

deep cells

YSL

Margin

Yolk cell

FGF

ERK2

epiboly

**Fig. 9.** Model for the distinct role for ERK1 and ERK2 during developmental cell migrations processes. (A) Represents the distinct effects of ERK1 and ERK2 knockdown on conversion-extension, as knockdown of ERK1 affected conversion to a greater extent, while the effect of ERK2 knockdown was more pronounced on extension. (B) Depicts the crucial role for FGF mediated ERK2 activation in the margin to initiate epiboly. Depletion of the active ERK2 signal from the margin by complete FGF inhibition or ERK2 knockdown prevents the blastomeres to initiate epiboly and subsequent gastrulation.

chemical inhibition of FGF signaling by SU5402 treatment (Fig. 8). Wild type embryos were dechorionated manually and treated with 40 μM SU5402 (Furthauer et al., 2004) from the 16-cell stage. Control embryos were treated with the same amount of DMSO solvent. The DMSO control embryos did not show any obvious phenotypes and initiated epiboly normally (Fig. 8A, ~100%). SU5402 treated embryos phenocopied severe ERK2 morphants (Fig. 8C) and did not initiate epiboly (Fig. 8B, ~85%, $n=84$ from two independent experiments). SU5402 treatment with lower concentration (20 μM) did not block epiboly.

To confirm the role of FGF signaling at the onset of epiboly and show the specificity, we also performed co-injections with mRNA encoding dominant negative FGF receptor 1 (XFD), dominant negative FGFR4 (bΔFR4) (Shinya et al., 2001) and the dominant negative H-Ras (RasN17). The injected embryos were scored for epiboly initiation (Fig. 8D), and embryos were subsequently analyzed for active ERK signal, by immuno-detection (dpERK). The observed dpERK phenotypes were classified in 4 groups; staining in the margin (black), depletion of dpERK from the margin, but still present at the putative dorsal side (light gray), no signal in the margin, but scattered pattern of cells expressing dpERK (dark gray) and no signal detected (white). The percentages of the different dpERK phenotypes ($n=30$ per condition) are represented in Fig. 8D. Injection of the various compounds did lower the levels of dpERK but none of these conditions showed the same phenotype on active ERK signaling as ERK2MO injection or SU5402 treatment (Fig. 8). In addition, we were not able to rescue embryos treated with saturating concentrations of SU5402 by co-injection of constitutively active forms of RAS (ca-Ras). Injection of ca-Ras can lead to early proliferation defects even before the epiboly arrest phenotype can be observed (Furthauer et al., 2002;Tsang et al., 2002), whereas injection of lower doses of ca-RAS did not rescue the epiboly arrest.

Together, our results provide evidence that mild knockdown of ERK1 and ERK2 affects CE movements differentially, without significantly altering early developmental patterning. ERK1 morphants showed a reduced convergence defect without a severe anterior–posterior extension defect, whereas ERK2 morphants did show a severe anterior–posterior extension defect without a significant convergence defect (Fig. 9A). Further analysis, using stronger knockdown conditions revealed that ERK2 is the active MAPK in the blastula margin. This indicates that the absence of this active ERK2 from the margin at the blastula to gastrula transition blocks the FGF mediated signaling that leads to initiation of epiboly. This subsequently prevents further progression of gastrulation cell migration processes, leading to an arrest in embryogenesis (Fig. 9B).

## Discussion

The ERK MAPKs are among the most studied signaling molecules, however the specificity of MAPKs in the developmental processes is not well understood. In this study we show that ERK1 and ERK2 have distinct roles in epiboly and CE movements during zebrafish embryogenesis. We present data demonstrating that ERK1 knockdown affects convergence to a larger extend, while ERK2 knockdown predominantly affects anterior–posterior extension during gastrulation cell migration processes (Fig. 9A). In addition, complete depletion of active ERK2 from the blastula margin prohibited proper cytoskeleton reorganization involved in epiboly initiation and led to an arrest of embryogenesis (Fig. 9B).

### Different lethality of ERK1 versus ERK2 knockdown

Morpholino knockdown of ERK1 and ERK2 resulted in a shorter body axis and affected somite shape. Knockdown of ERK2 also disrupted the formation of the MHB and was more lethal than knockdown of ERK1 (Fig. 1). This is in agreement with gene targeting results in mice showing that *erk1−/−* mice are viable and without embryonic phenotypes, whereas *erk2−/−* mice are lethal (Pagès et al., 1999). In zebrafish, the same amount of *erk2* mRNA that rescued morpholino knockdown of ERK2 was also able to cross-rescue knockdown of ERK1. In contrast, the *erk1* mRNA could not cross-rescue ERK2 morphants. Our results support the suggestion of Yao et al. that ERK2 can compensate for the loss of ERK1 (Yao et al., 2003; Saba-El-Leil et al., 2003). In addition, double ERK1 and ERK2 knockdown does not completely synergize to phenocopy the stronger knockdown conditions of ERK2, indicating distinct functions for ERK1 and ERK2. The difference between the observed developmental defects and lethality in zebrafish ERK1 morphants and the lack of a severe phenotype in *erk1−/−* mice (Mazzucchelli et al., 2002) is remarkable and suggests different redundancy and adaptation mechanisms in these organisms.

### Distinct roles for ERK1 and ERK2 in convergence and extension cell movements during gastrulation

Phenotypes of surviving ERK1 and ERK2 morphants indicated possible effects in CE cell movements. In situ hybridization using combinations of markers for these processes supported this hypothesis (Fig. 2), while in situ hybridization experiments with patterning marker genes did not show a significant altering of the early cell fate specification (Fig. S3). Indications for distinct loss-of-function defects of ERK1 versus ERK2 knockdown on CE cell movements during gastrulation were directly addressed by cell-tracing experiment in ERK1 and ERK2 morphants (Fig. 3). We found that CE movements were differently affected upon ERK1 versus ERK2 knockdown as ERK1 morphants showed a convergence defect without a severe posterior-extension defect, whereas ERK2 morphants showed a more severe reduction in anterior–posterior extension, pointing towards different downstream targets of ERK1 and ERK2 and divergence of ERK

signaling at this level. The study of Pullikuth et al. supports our finding that ERK1 also is involved in cell migration processes, as they show that the ERK1 specific scaffold protein MP1, and its partner p14 are required for Rho/Rho kinase functions, involved in the turnover of cell adhesions and cytoskeleton rearrangements important for cell motility of REF52 fibroblasts (Pullikuth et al., 2005).

CE movements during zebrafish gastrulation involve different cellular events depending on the position of the cells along the dorso-ventral axis (Myers et al., 2002). Dorsal convergence appears to require migration of cells on the extracellular matrix, while extension movements might be dependent on cell–cell adhesion, involving neighboring cells crawling over the surfaces of the surrounding cells. Importantly, studies in zebrafish demonstrated that convergence and extension cell movements may be considered as separate morphogenetic movements of gastrulation cell migration in zebrafish (Glickman et al., 2003; Bakkers et al., 2004; Daggett et al., 2004). In other model systems interaction between ERK signaling and cell migration during gastrulation was also observed (Bottcher and Niehrs, 2005).

*Epiboly initiation requires active/phosphorylated ERK2 in the blastula margin*

Saturating knockdown conditions were applied to address the possible functions of ERK1 and ERK2 in epiboly initiation, since phosphorylated ERKs were previously detected in the blastula margin (Fig. S1). The increased knockdown of ERK1 only slightly delayed epiboly, whereas 84% of the ERK2MO injected embryos did not initiate epiboly at all. Immuno-histochemical studies on ERK1 and ERK2 morphants using a phospho-ERK antibody showed that ERK2 is specifically activated in the blastula margin (Fig. 5) and crucial for epiboly progression. Our results indicate that depletion of this active ERK2 from the margin prevents cells from the animal pole to migrate over the yolk–cell at the onset of epiboly (Fig. 6). In addition, migration of the YSL to the vegetal pole was prevented (Fig. 7), thereby removing one of the motors for gastrulation movements (Solnica-Krezel and Driever, 1994; D'Amico and Cooper, 2001; Solnica-Krezel, 2006).

The impaired epiboly in ERK2 morphant embryos is accompanied by severe mesoderm induction defects (Fig. 6). To exclude that the epiboly defect is just due to defected mesoderm development rather than specific defects in morphogenesis, we demonstrated that transplanted cells from severe ERK-morphants into a wild type background were still able to undergo epiboly with reduced cell migration efficiency. Importantly, it has been described that epiblast and hypoblast layers can move independently. For instance, in maternal-zygotic *one-eyed pinhead* mutant embryos, which lack hypoblast cells, epiblast cells still epibolize properly (Hammerschmidt et al., 1996). This indicates that the observed epiboly arrest in ERK2 morphants likely is not due to defected mesoderm formation, but is caused by defects in cell migration and cytoskeleton reorganization.

*FGFs act as activators of ERK2 in the blastula margin*

Our results suggest that activation of ERK2 plays a major role in early epiboly initiation. The question remains which signaling cascade that regulates the onset of epiboly, is blocked by ERK2 knockdown. At the upstream signaling level multiple interconnected signaling pathways, such as Nodal, Wnt, BMP and FGF, act together to coordinate epiboly and gastrulation processes (Schier, and T.W.S., 2005) and are therefore possibly connected with ERK2 activation. In *Drosophila*, *Xenopus*, mouse and zebrafish, the functions of ERK MAPKs are often related to FGF signaling. In the early mouse gastrula, FGFs are required for the migration of the epiblast cells out of the primitive streak (Sun et al., 1999). In chicken, FGFs signal as chemotactic cues during gastrulation, and coordinate cell movements during ingression of the epiblast cells through the primitive streak (Yang et al., 2002). During

early mesoderm migration in *Drosophila*, the local MAPK activation pattern suggests that the FGF receptor (Htl) is specifically activated at the leading edge of the migrating mesoderm cells (Gabay et al., 1997; Gryzik and Muller, 2004). In zebrafish development, activated ERK proteins are localized in overlapping expression regions with various FGF ligands and other components of the FGF pathway (Fig. S1) (Pozios et al., 2001; Sawada et al., 2001; Furthauer et al., 2002; Tsang et al., 2002; Poulain et al., 2006). In previous studies inhibition of the FGF pathway resulted in tailless phenotypes, similar to ERK1 and ERK2 morphants (Figs. 1 and S6) (Griffin et al., 1995; Draper et al., 2003; Griffin and Kimelman, 2003; Mathieu et al., 2004). Therefore we examined the involvement of FGF signaling at the onset of epiboly by the use of several inhibitors of the FGF/Ras/MAPK signaling cascade. Saturated inhibition of FGF signaling by SU5402 treatment resulted in complete phenocopy of ERK2 morphant phenotypes (Fig. 8), demonstrating for the first time an important role for FGF-mediated ERK2 activation at the onset of epiboly. Injection of dominant negative FGFR1 or dominant negative hRas (N17) only, or co-injection of dnFGFR1 with dnFGFR4 (bΔFR4) led to diminishing of active ERK2 signal, without affecting epiboly initiation. This suggests more genes of the FGF family or different signaling processes to be involved. It has been described that FGFR signaling involves activation of multiple downstream signaling cascades (Coumoul and Deng, 2003; Bottcher and Niehrs, 2005; Thisse and Thisse, 2005). For instance, using different chemical strategies to inhibit phosphatidylinosito-3 kinase signaling during *Xenopus* mesoderm inductions, it was shown that PI3K can act in parallel to ERK signaling in response to FGF (Carballada et al., 2001). Studies using the ascidian *Ciona* demonstrate that the phenotypical outcome of chemical inhibition of FGF signaling depends on the timing of drug application (Kim and Nishida, 2001). Attempts by other labs to block FGF signaling by triple knockdown of FGF8,17b and 24 in zebrafish did not inhibit epiboly initiation (Raible and Brand, 2001; Draper et al., 2003; Furthauer et al., 2004; Tsang et al., 2004; Poulain et al., 2006), indicating the complexity of this process.

*ERK signaling is essential for effective actin accumulation at the EVL and microtubule reorganization in the YSL during epiboly*

In the next course of our study we addressed the question how ERK2 signaling controls epiboly progression and integrates with cytoskeleton reorganization at the onset of gastrulation cell movements. The migration of the YSN to the vegetal pole is considered as a driving force through all stages of epiboly (Kane et al., 1996), next to radial intercalation (Myers et al., 2002; Montero and Heisenberg, 2004; Solnica-Krezel, 2006). At late blastula stages, the YSL forms a broad band and contains most of the yolk syncytial nuclei (YSN). At sphere stage, the YSN of the YSL crowd into one plain to initiate epiboly. This process is mediated by the microtubule network of the external YSL, which contracts and becomes denser at the margin (Solnica-Krezel and Driever, 1994), thereby aligning the YSN lateral to the blastula margin. Depletion of ERK2 severely affects this microtubule mediated process and the YSN do not migrate to the vegetal pole. In vitro studies showed that active ERK is involved in microtubule destabilization (Harrison and Turley, 2001). Therefore the loss of ERK signaling is likely to disturb microtubule stability in the YSL as we observed in our knockdown study.

The movement of the EVL over the yolk surface involves the constriction of marginal cells, a process that depends on the recruitment of actin and myosin2 along the margin of the EVL (Köppen et al., 2006). The recruitment of actin to the margin was not observed in ERK2 morphants, suggesting a mechanism why the EVL of ERK2 morphants did not go into epiboly (Fig. 8). A possible mechanistic link between ERK1/2 signaling and actin reorganization might be mediated by Paxillin. Paxillin is a focal-adhesion adaptor involved in focal-adhesion dynamics and cell migration (Turner, 2000). The direct upstream ERK-activator MEK is constitutively associated with Paxillin

and extracellular stimuli induce the binding of active RAF and inactive ERK to Paxillin to mediate ERK activation at focal complexes, therefore Paxillin can serve as an ERK-regulated scaffold for coordinated FAK and Rac activation in epithelial morphogenesis (Ishibe et al., 2004). In zebrafish, activated Paxillin, focal-adhesion kinase (FAK), and cadherin co-distribute at the lateral membranes of the EVL during early morphogenesis (Crawford et al., 2003). In this study we found elevated levels of phosphorylated ERK within the EVL and even stronger signals at the margin to yolk interface, allowing for speculation that active ERK signaling is involved in focal-adhesion assembly and disassembly between the EVL and YSL, but its precise role and the mechanism should be clarified or confirmed by further studies. Together, we conclude that the absence of microtubule-dependent migration of the YSN and actin-reorganization defects by ERK2 knockdown contributes to the developmental arrest at the blastula to gastrula transition.

A number of mutants described for epiboly arrest show delayed or arrested epiboly at later stages, but not a block at blastula to gastrula transition (Kane et al., 1996). For example, different *hab* alleles, containing mutations in the cell adhesion molecule E-cadherin (*cdh1*), arrest epiboly of deep cells at mid-gastrulation, whereas epiboly of EVL and YSL proceeds further (Kane et al., 2005; Shimizu et al., 2005). Reduction of E-cadherin protein levels by morpholino knockdown also delayed epiboly and affected intercalation and possibly extension cell migration (Kane et al., 2005). Stronger loss of E-cadherin function impaired epiboly at earlier stages (Babb and Marrs, 2004), similar as observed in our study of ERK2 morphants. The morphological changes characteristic for an EMT-like transition; cytoskeleton reorganization and disruption of cell junctions are however, independent of cadherin switching. This indicates that the developmental defects in the morphants are caused defects on multiple levels. An interesting link is starting to emerge between activation of ERK MAPKs via hepatocyte growth factors and the regulation of E-cadherin expression via *snail* in cancer processes (Medici et al., 2006; Grotegut et al., 2006). In future studies we would like to address the link of ERK MAPK with FGF, E-cadherin and other signaling components using micro-array analyses in the different ERK knockdown backgrounds, and address the molecular mechanism of ERK activation integrates with cytoskeleton reorganization required for gastrulation cell movements.

## Acknowledgments

## Appendix A. Supplementary data

Supplementary data associated with this article can be found, in the online version, at doi:10.1016/j.ydbio.2008.04.032.

## References

Babb, S.G., Marrs, J.A., 2004. E-cadherin regulates cell movements and tissue formation in early zebrafish embryos. Dev. Dyn. 230, 263–277.
Bakkers, J., Kramer, C., Pothof, J., Quaedvlieg, N.E.M., Spaink, H.P., Hammerschmidt, M., 2004. Has2 is required upstream of Rac1 to govern dorsal migration of lateral cells during zebrafish gastrulation. Development 131, 525–537.
Betchaku, T., Trinkaus, J.P., 1978. Contact relations, surface-activity, and cortical microfilaments of marginal cells of enveloping layer and of yolk syncytial and yolk cytoplasmic layers of *Fundulus* before and during epiboly. J. Exp. Zool. 206, 381–426.
Bottcher, R.T., Niehrs, C., 2005. Fibroblast growth factor signaling during early vertebrate development. Endocr. Rev. 26, 63–77.
Carballada, R., Yasuo, H., Lemaire, P., 2001. Phosphatidylinositol-3 kinase acts in parallel to the ERK MAP kinase in the FGF pathway during *Xenopus* mesoderm induction. Development 128, 35–44.
Cheng, J.C., Miller, A.L., Webb, S.E., 2004. Organization and function of microfilaments during late epiboly in zebrafish embryos. Dev. Dyn. 231, 313–323.
Corson, L.B., Yamanaka, Y., Lai, K.M.V., Rossant, J., 2003. Spatial and temporal patterns of ERK signaling during mouse embryogenesis. Development 130, 4527–4537.
Coumoul, X., Deng, C.-X., 2003. Roles of FGF receptors in mammalian development and congenital diseases. Birth Defects Res. (Part C) 69 (4), 286–304.
Crawford, B.D., Henry, C.A., Clason, T.A., Becker, A.L., Hille, M.B., 2003. Activity and distribution of paxillin, focal adhesion kinase, and cadherin indicate cooperative roles during zebrafish morphogenesis. Mol. Biol. Cell 14, 3065–3081.
D'Amico, L.A., Cooper, M.S., 2001. Morphogenetic domains in the yolk syncytial layer of axiating zebrafish embryos. Dev. Dyn. 222, 611–624.
Daggett, D.F., Boyd, C.A., Gautier, P., Bryson-Richardson, R.J., Thisse, C., Thisse, B., Amacher, S.L., Currie, P.D., 2004. Developmentally restricted actin-regulatory molecules control morphogenetic cell movements in the zebrafish gastrula. Curr. Biol. 14, 1632–1638.
Delfini, M.C., Dubrulle, J., Malapert, P., Chal, J., Pourquie, O., 2005. Control of the segmentation process by graded MAPK/ERK activation in the chick embryo. PNAS 102, 11343–11348.
Deng, T., Karin, M., 1994. c-Fos transcriptional activity stimulated by H-Ras-activated protein kinase distinct from JNK and ERK. Nature 371, 171–175.
Draper, B.W., Stock, D.W., Kimmel, C.B., 2003. Zebrafish fgf24 functions with fgf8 to promote posterior mesodermal development. Development 130, 4639–4654.
Furthauer, M., Lin, W., Ang, S.L., Thisse, B., Thisse, C., 2002. Sef is a feedback-induced antagonist of Ras/MAPK-mediated FGF signalling. Nat. Cell Biol. 4, 170–174.
Furthauer, M., Van Celst, J., Thisse, C., Thisse, B., 2004. Fgf signalling controls the dorsoventral patterning of the zebrafish embryo. Development 131, 2853–2864.
Gabay, L., Seger, R., Shilo, B.Z., 1997. MAP kinase in situ activation atlas during *Drosophila* embryogenesis. Development 124, 3535–3541.
Pagès, Gilles, Guérin, Sandrine, Grall, Dominique, Bonino, Frédéric, Smith, Austin, Anjuere, Fabienne, Auberger, Patrick, Pouysségur, Jacques, 1999. Defective thymocyte maturation in p44 MAP kinase (Erk 1) knockout mice. Science 286, 1374–1377.
Glickman, N.S., Kimmel, C.B., Jones, M.A., Adams, R.J., 2003. Shaping the zebrafish notochord. Development 130, 873–887.
Gotoh, Y., Masuyama, N., Suzuki, A., Ueno, N., Nishida, E., 1995. Involvement of the map kinase cascade in *Xenopus* mesoderm induction. Embo J. 14, 2491–2498.
Griffin, K.J.P., Kimelman, D., 2003. Interplay between FGF, one-eyed pinhead, and T-box transcription factors during zebrafish posterior development. Dev. Biol. 264, 456–466.
Griffin, K., Patient, R., Holder, N., 1995. Analysis of FGF function in normal and no tail zebrafish embryos reveals separate mechanisms for formation of the trunk and the tail. Development 121, 2983–2994.
Grotegut, S., von Schweinitz, D., Christofori, G., Lehembre, F., 2006. Hepatocyte growth factor induces cell scattering through MAPK/Egr-1-mediated upregulation of Snail1. Embo J. 25, 3534–3545.
Gryzik, T., Muller, H.A.J., 2004. FGF8-like1 and FGF8-like2 encode putative ligands of the FGF receptor Htl for mesoderm migration and are required in the *Drosophila* gastrula. Curr. Biol. 14, 659–667.
Hammerschmidt, M., Pelegri, F., Mullins, M.C., Kane, D.A., Brand, M., vanEeden, F.J.M., FurutaniSeiki, M., Granato, M., Haffter, P., Heisenberg, C.P., Jiang, Y.J., Kelsh, R.N., Odenthal, J., Warga, R.M., NussleinVolhard, C., 1996. Mutations affecting morphogenesis during gastrulation and tail formation in the zebrafish, *Danio rerio*. Development 123, 143–151.
Harrison, R.E., Turley, E.A., 2001. Active erk regulates microtubule stability in H-ras-transformed cells. Neoplasia 3, 385–394.
Hongo, I., Kengaku, M., Okamoto, H., 1999. FGF signaling and the anterior neural induction in *Xenopus*. Dev. Biol. 216, 561–581.
Ishibe, S., Joly, D., Liu, Z.X., Cantley, L.G., 2004. Paxillin serves as an ERK-regulated scaffold for coordinating FAK and Rac activation in epithelial morphogenesis. Mol. Cell 16, 257–267.
Johnson, G.L., Lapadat, R., 2002. Mitogen-activated protein kinase pathways mediated by ERK, JNK, and p38 protein kinases. Science 298, 1911–1912.
Johnson, G.L., Dohlman, H.G., Graves, L.M., 2005. MAPK kinase kinases (MKKKs) as a target class for small-molecule inhibition to modulate signaling networks and gene expression. Curr. Opin. Chem. Biol. 9, 325–331.
Jopling, C., den Hertog, J., 2005. Fyn/Yes and non-canonical Wnt signalling converge on RhoA in vertebrate gastrulation cell movements. Embo Rep. 6, 426–431.
Kane, D.A., Hammerschmidt, M., Mullins, M.C., Maischein, H.M., Brand, M., van Eeden, F.J., Furutani-Seiki, M., Granato, M., Haffter, P., Heisenberg, C.P., Jiang, Y.J., Kelsh, R.N., Odenthal, J., Warga, R.M., Nusslein-Volhard, C., 1996. The zebrafish epiboly mutants. Development 123, 47–55.
Kane, D.A., McFarland, K.N., Warga, R.M., 2005. Mutations in half baked/E-cadherin block cell behaviors that are necessary for teleost epiboly. Development 132, 1105–1116.
Kato, T., Ohtani-kaneko, R., Ono, K., Okado, N., Shiga, T., 2005. Developmental regulation of activated ERK expression in the spinal cord and dorsal root ganglion of the chick embryo. Neurosci. Res. 52, 11–19.

Kim, G.J., Nishida, H., 2001. Role of the FGF and MEK signaling pathway in the ascidian embryo. Dev. Growth Differ. 43, 521–533.

Kolch, W., 2005. Coordinating ERK/MAPK signalling through scaffolds and inhibitors. Nat. Rev. Mol. Cell Biol. 6, 827–837.

Köppen, M., Fernandez, B.G., Carvalho, L., Jacinto, A., Heisenberg, C.P., 2006. Coordinated cell-shape changes control epithelial movement in zebrafish and *Drosophila*. Development 133, 2671–2681.

Kozlowski, D.J., Murakami, T., Ho, R.K., Weinberg, E.S., 1997. Regional cell movement and tissue patterning in the zebrafish embryo revealed by fate mapping with caged fluorescein. Biochem. Cell Biol.-Biochimie et Biologie Cellulaire 75, 551–562.

Krens, S.F.G., He, S., Spaink, H.P., Snaar-Jagalska, B.E., 2006. Characterization and expression patterns of the MAPK family in zebrafish. Gene Expr. Patterns 6, 1019–1026.

LaBonne, C., Burke, B., Whitman, M., 1995. Role of MAP kinase in mesoderm induction and axial patterning during *Xenopus* development. Development 121, 1475–1486.

Lloyd, A., 2006. Distinct functions for ERKs? J. Biol. 5, 13.

Mathieu, J., Griffin, K., Herbomel, P., Dickmeis, T., Strahle, U., Kimelman, D., Rosa, F.M., Peyrieras, N., 2004. Nodal and Fgf pathways interact through a positive regulatory loop and synergize to maintain mesodermal cell populations. Development 131, 629–641.

Mazzucchelli, C., Vantaggiato, C., Ciamei, A., Fasano, S., Pakhotin, P., Krezel, W., Welzl, H., Wolfer, D.P., Pages, G., Valverde, O., 2002. Knockout of ERK1 MAP kinase enhances synaptic plasticity in the striatum and facilitates striatal-mediated learning and memory. Neuron 34, 807–820.

Medici, D., Hay, E.D., Goodenough, D.A., 2006. Cooperation between snail and LEF-1 transcription factors is essential for TGF-beta 1-induced epithelial-mesenchymal transition. Mol. Biol. Cell 17, 1871–1879.

Mohammadi, M., McMahon, G., Sun, L., Tang, C., Hirth, P., Yeh, B.K., Hubbard, S.R., Schlessinger, J., 1997. Structures of the tyrosine kinase domain of fibroblast growth factor receptor in complex with inhibitors. Science 276, 955–960.

Montero, J.A., Heisenberg, C.P., 2004. Gastrulation dynamics: cells move into focus. Trends Cell Biol. 14, 620–627.

Myers, D.C., Sepich, D.S., Solnica-Krezel, L., 2002. Convergence and extension in vertebrate gastrulae: cell movements according to or in search of identity? Trends Genet. 18, 447–455.

Ornitz, D., Itoh, N., 2001. Fibroblast growth factors. Genome Biol., 2, reviews 3005. 1-3005.

Poulain, M., Furthauer, M., Thisse, B., Thisse, C., Lepage, T., 2006. Zebrafish endoderm formation is regulated by combinatorial Nodal, FGF and BMP signalling. Development 133, 2189–2200.

Pozios, K.C., Ding, J., Degger, B., Upton, Z., Duan, C., 2001. IGFs stimulate zebrafish cell proliferation by activating MAP kinase and PI3-kinase-signaling pathways. Am. J. Physiol. Regul. Integr. Comp. Physiol. 280, R1230–R1239.

Pullikuth, A., McKinnon, E., Schaeffer, H.J., Catling, A.D., 2005. The MEK1 scaffolding protein MP1 regulates cell spreading by integrating PAK1 and Rho signals. Mol. Cell. Biol. 25, 5119–5133.

Raible, F., Brand, M., 2001. Tight transcriptional control of the ETS domain factors Erm and Pea3 by Fgf signaling during early zebrafish development. Mech. Dev. 107, 105–117.

Saba-El-Leil, M.K., Vella, F.D.J., Vernay, B., Voisin, L., Chen, L., Labrecque, N., Ang, S.L., Meloche, S., 2003. An essential function of the mitogen-activated protein kinase Erk2 in mouse trophoblast development. Embo Rep. 4, 964–968.

Sawada, A., Shinya, M., Jiang, Y.J., Kawakami, A., Kuroiwa, A., Takeda, H., 2001. Fgf/MAPK signalling is a crucial positional cue in somite boundary formation. Development 128, 4873–4880.

Schier, A.F., T.W.S., 2005. Molecular genetics of axis formation in zebrafish. Annu. Rev. Genet. 39, 561–613 12-15-2005.

Sepich, D.S., Myers, D.C., Short, R., Topczewski, J., Marlow, F., Solnica-Krezel, L., 2000. Role of the zebrafish trilobite locus in gastrulation movements of convergence and extension. Genesis 27, 159–173.

Shimizu, T., Yabe, T., Muraoka, O., Yonemura, S., Aramaki, S., Hatta, K., Bae, Y.K., Nojima, H., Hibi, M., 2005. E-cadherin is required for gastrulation cell movements in zebrafish. Mech. Dev. 122, 747–763.

Shinya, M., Koshida, S., Sawada, A., Kuroiwa, A., Takeda, H., 2001. Fgf signalling through MAPK cascade is required for development of the subpallial telencephalon in zebrafish embryos. Development 128, 4153–4164.

Snaar-Jagalska, B.E., Krens, S.F.G., Robina, I., Wang, L.X., Spaink, H.P., 2003. Specific activation of ERK pathways by chitin oligosaccharides in embryonic zebrafish cell lines. Glycobiology 13, 725–732.

Solnica-Krezel, L., 2006. Gastrulation in zebrafish — all just about adhesion? Curr. Opin. Genet. Dev. 16, 433–441.

Solnica-Krezel, L., Driever, W., 1994. Microtubule arrays of the zebrafish yolk cell: organization and function during epiboly. Development 120, 2443–2455.

Stathopoulos, A., Tam, B., Ronshaugen, M., Frasch, M., Levine, M., 2004. pyramus and thisbe: FGF genes that pattern the mesoderm of *Drosophila* embryos. Genes Dev. 18, 687–699.

Sun, X., Meyers, E.N., Lewandoski, M., Martin, G.R., 1999. Targeted disruption of Fgf8 causes failure of cell migration in the gastrulating mouse embryo. Genes Dev. 13, 1834–1846.

Thisse, B., Thisse, C., 2005. Functions and regulations of fibroblast growth factor signaling during embryonic development. Dev. Biol. 287, 390–402.

Thisse, C., Thisse, B., Schilling, T.F., Postlethwait, J.H., 1993. Structure of the zebrafish snail1 gene and its expression in wild-type, spadetail and no tail mutant embryos. Development 119, 1203–1215.

Tsang, M., Friesel, R., Kudoh, T., Dawid, I.B., 2002. Identification of Sef, a novel modulator of FGF signalling. Nat. Cell Biol. 4, 165–169.

Tsang, M., Maegawa, S., Kiang, A., Habas, R., Weinberg, E., Dawid, I.B., 2004. A role for MKP3 in axial patterning of the zebrafish embryo. Development 131, 2769–2779.

Turner, C.E., 2000. Paxillin interactions. J. Cell Sci. 113, 4139–4140.

Umbhauer, M., Marshall, C.J., Mason, C.S., Old, R.W., Smith, J.C., 1995. Mesoderm induction in *Xenopus* caused by activation of Map kinase. Nature 376, 58–62.

Uzgare, A.R., Uzman, J.A., El Hodiri, H.M., Sater, A.K., 1998. Mitogen-activated protein kinase and neural specification in *Xenopus*. PNAS 95, 14833–14838.

Vantaggiato, C., Formentini, I., Bondanza, A., Bonini, C., Naldini, L., Brambilla, R., 2006. ERK1 and ERK2 mitogen-activated protein kinases affect Ras-dependent cell signaling differentially. J. Biol. 5 (5), 14.1–14.15.

Wilson, R., Vogelsang, E., Leptin, M., 2005. FGF signalling and the mechanism of mesoderm spreading in *Drosophila* embryos. Development 132, 491–501.

Yang, X., Dormann, D., Munsterberg, A.E., Weijer, C.J., 2002. Cell movement patterns during gastrulation in the chick are controlled by positive and negative chemotaxis mediated by FGF4 and FGF8. Dev. Cell 3, 425–437.

Yao, Y., Li, W., Wu, J., Germann, U.A., Su, M.S.S., Kuida, K., Boucher, D.M., 2003. Extracellular signal-regulated kinase 2 is necessary for mesoderm differentiation. PNAS 100, 12759–12764.